Inorganic Chemistry

Article

pubs.acs.org/IC

Improving SERS Activity of Inositol Hexaphosphate Capped Silver Nanoparticles: Fe^{3+} as a Switcher

Xiaoyu Guo, Yichen Fu, Shuyue Fu, Hui Wang, Tianxi Yang, Ying Wen, and Haifeng Yang*

Department of Chemistry, Key Laboratory of Resource Chemistry of Ministry of Education, Shanghai Key Laboratory of Rare Earth Functional Materials, Shanghai Normal University, 100 Guilin Road, Shanghai 200234, People's Republic of China

Supporting Information

ABSTRACT: Inositol hexaphosphate (IP_6) capped silver nanoparticles (IP_6@AgNPs) were fabricated as surface-enhanced Raman scattering (SERS) active substrates. SERS activity of IP_6@AgNPs could be further improved via adding due amounts of Fe^{3+} to form Fe^{3+}–IP_6@AgNPs. The mechanism of Fe^{3+}-induced SERS improvement of IP_6@AgNPs can be attributed to the strong interaction of IP_6 and Fe^{3+}, which leads to controllable adjustment of the gap among neighboring nanoparticles to produce "hot spots". The above mechanism was confirmed with ultraviolet–visible (UV-vis) spectroscopy, transmission electron microscope (TEM), dynamic light scattering (DLS), Fourier transform infrared (FT-IR) spectroscopy, and X-ray photoelectron spectroscopy (XPS). Such Fe^{3+}–IP_6@AgNPs-based SERS system was used to detect Rhodamine 6G (R6G) down to the trace level of 10^{-10} mol L^{-1}. Besides, New Fuchsin (NF) was also used as a Raman probe to calculate the enhancement factor (EF) of IP_6@AgNPs without and with Fe^{3+}. The SERS activity of IP_6@AgNPs happened extreme decrease after one–year storage and could be recovered to great extent aided by the addition of Fe^{3+}. The Fe^{3+} optimized IP_6@AgNPs system could be applied to detect thymine at trace level by SERS.

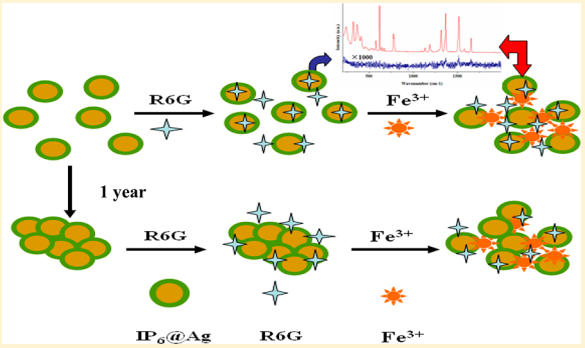

1. INTRODUCTION

Surface-enhanced Raman scattering (SERS) was first observed from the experiment of pyridine adsorbed on the electrochemically roughened Ag electrode in 1974.[1] Since then, SERS technique has been concerned and employed for trace detection, because of its high sensitivity and molecular information.[2−15] Nowadays, a long-range electromagnetic (EM) effect mechanism has been widely accepted by most researchers, resulting from light exciting surface plasmon resonance of some rough metallic surface at nanoscale causing the local EM field enhancement.[16−19] Extremely strong local electromagnetic field enhancement of some suitably aggregated metal nanoparticles called "hot spot", improves SERS detection sensitivity to single molecular level.[20−22] For example, Brus et al.[23] studied the single-molecule SERS and found that the isolated nanoparticles only brought litter enhancement for Raman intensity, but the aggregates with multiple particles induced large enhancement. Based on the phenomenon, they concluded that the active sites were likely located at the junction of two or more metal nanoparticles due to huge electromagnetic field enhancements produced by plasmon coupling between nanoparticles. Li et al.[24] showed that a huge enhancement factor was provided from the molecules between the closed nano–fingertips, which produced plenty of "hot spots".

As is well-known, metal colloids, normally silver and gold nanoparticles with a high enhancement factor,[3,25,26] are used for the SERS-active substrates and they are easy to be prepared. Beyond that, making "hot spots" among metal nanoparticles could be controlled by adding some agents. Li et al.[27] prepared highly active SERS substrate using ethanol as inductive agent, which preferential dissolution of CTAB from its capped silver nanoparticles (AgNPs), leading closer gap between AgNPs and the formation of aggregates with more "hot spots". In addition, Ahonen et al.[28] fabricated the aggregation of AgNPs using a dithiol crosslinker. Lu et al.[29] produced AgNP aggregates via the aid of HNO_3 as an aggregating agent. Hu et al.[30] prepared an aggregated AgNP film using sodium chloride. Chen et al.[31] prepared aggregation of 4-MPY functionalized AgNPs using protamine as a medium. Such agents that could induce the aggregation of metal nanoparticles and tune their SERS activity are called SERS switchers. Alternatively, another idea for easily producing "hot spots" is to choose the right capping agent to introduce the attractive force within the nanoparticles. Inositol hexakisphosphate (IP_6) containing six phosphates as an agent that is nontoxic to humans and "green" to the environment has a strong capability of chelating with metal ions.[32] Inspired by the tense interaction of metal ions and IP_6, we used IP_6 as the crosslinker to cap Ag colloids[33] and tried to employ trivalent iron ion as a SERS switcher to tune the gap between the IP_6@AgNPs to increase the amount of "hot spots" for elevating their

Received: February 17, 2014
Published: July 10, 2014

   dx.doi.org/10.1021/ic5003836 | Inorg. Chem. 2014, 53, 7227−7232

SERS activity. In the present method, as a key innovation, the mechanism of Fe^{3+}-optimized SERS activity of IP_6@AgNPs was investigated with UV-vis spectroscopy, transmission electron microscope (TEM), dynamic light scattering (DLS), Fourier transform infrared spectroscopy (FTIR), and X-ray photoelectron spectroscopy (XPS). Rhodamine 6G (R6G) and New Fuchsin (NF) were used as Raman probe to investigate the SERS activity of Fe^{3+}−IP_6@AgNPs.

Thymine as one of the four nucleic acid bases plays important role in genetic expression and replications. In addition, the high photoreactivity of thymine exhibits the adsorption of ultraviolet light leading to the creation of a cyclobutane dimer.[34,35] Routinely, the analysis of low-concentration thymine is conducted by high-performance liquid chromatography (HPLC) but it involves high reagent cost and is time-consuming.[36] We present Fe^{3+}−IP_6@AgNPs-based SERS method as a fast and sensitive tool might be developed for the detection of low-concentration thymine in this work.

Furthermore, after a storage term as long as one year under room temperature, the dramatic decrease of SERS activity of IP_6@AgNPs was observed. We found that adding the proper amount of Fe^{3+} into the aged IP_6@AgNPs, their SERS could be refreshed to great extent. This Fe^{3+}−IP_6@AgNPs-based SERS protocol might be extended to detect other biomolecules.

2. EXPERIMENTAL METHODS

2.1. Materials. All chemicals were of analytical grade or the highest purity available. Silver nitrate ($AgNO_3$), trisodium citrate, thymine, rhodamine 6G, and inositol hexaphosphate (IP_6) in Na−salt form (dodecasodium of phytic acid) were obtained from Sigma−Aldrich (USA). New Fuchsin (NF) and $FeCl_3{\cdot}6H_2O$ were obtained from Sinopharm Chemical Reagent, Shanghai, China. The concentration of 10 mM Fe^{3+} stock solution was prepared with $FeCl_3{\cdot}6H_2O$. Milli-Q water (18.2 MΩ cm) was obtained using a Milli-Q system (Millipore). Glassware was embathed in aqua regia and then thoroughly washed with Milli-Q water.

2.2. Preparation of SERS Substrates. The IP_6 capped AgNPs were prepared by a method similar to a previously reported method.[33] Five milliliters (5 mL) of 0.001 M IP_6 solution was added to 150 mL 0.001 M silver nitrate solution. After the solution was heated to boiling, 3 mL of 1% tri-sodium citrate solution was added slowly under vigorous stirring. The reaction of the solution kept 6 h under boiling temperature to obtain the product Ag colloid. A due amount of Milli-Q water was added to obtain 125 mL of Ag colloid (the final concentration of Ag was 1.2 mM). As a comparison, AgNPs were also synthesized following the method reported by Lee and Meisel.[37]

Twenty microliters (20 μL) Ag colloid solution was taken out, and then 10 μL of Fe^{3+} with varying concentrations from 0 to 1400 μM was added. The mixture was shocked on Lab dancer for 20 s to obtain the improved SERS-active substrates denoted as Fe^{3+}−IP_6@AgNPs.

2.3. SERS Measurement. R6G solution was diluted to various stock concentrations ranging from 1×10^{-6} M to 1×10^{-9} M using Milli-Q water, and then 10 μL of R6G solution with different concentration was mixed with 30 μL of Fe^{3+}−IP_6@AgNPs solution. After shocking on Lab dancer for 20 s, the above mixture was taken into the capillary tube for the detection by focusing laser spot from confocal Raman system. Raman data of NF molecule was measured to calculate the enhancement factor. The process of data collecting was the same as R6G. SERS measurement for thymine was performed with the same process. In the case of stability investigation, IP_6@AgNPs stored for 1 year at room temperature was used to conduct SERS measurement. In turn, SERS result was also recorded after adding Fe^{3+} into IP_6@AgNPs and R6G (1×10^{-6} M) for observing the SERS activity recovery of IP_6@AgNPs.

2.4. Instrumentation. UV-vis spectrum of colloid was collected using a Model 760-CRT double-beam spectrophotometer (Shanghai Precision and Scientific Instrument Co., Ltd.). The morphology and distribution of the colloid were measured with a Model JEM-2100EXII transmission electron microscope (JEOL Co., Ltd.), operating at 200 kV. Fourier transform infrared spectroscopy (FT−IR) was detected using a Nicolet infrared spectrometer (AVATAR-370-FTIR), using a KBr compression process method. X-ray photoelectron spectroscopy (XPS; Model PHI 5000, Versa Probe) was performed to identify the chemical composition of the observed nanocomposites. The dynamic light scattering (DLS) was measured using a Malvern Zetasizer Nano ZS model ZEN3600 (Worcestershire, U.K.) equipped with a standard 633-nm laser. SERS spectra were recorded using a Jobin Yvon confocal laser Raman system (SuperLabRam II), which was equipped with a He−Ne laser at 632.8 nm with a power of ca. 5 mW. Each spectrum was obtained by three accumulations, and the acquisition time in each case was typically 10 s. The mixture was shocked using Lab dancer (IKA) and the rotating speed is fixed at 2800 rpm.

3. RESULTS AND DISCUSSION

3.1. Mechanism of Raman Enhancement of Fe^{3+}−IP_6@AgNPs. UV-vis spectra of IP_6@AgNPs and Fe^{3+}−IP_6@AgNPs are shown in Figure 1. TEM experiments were also conducted

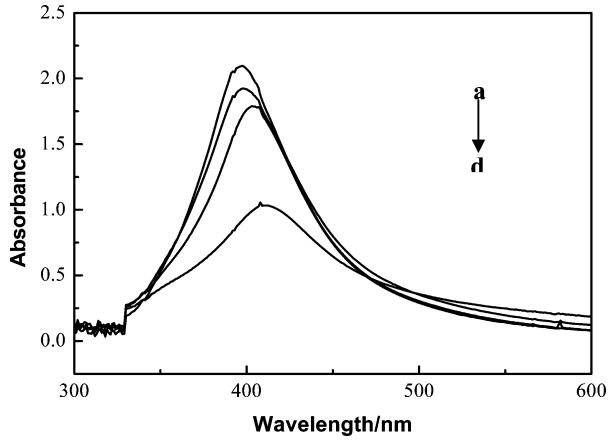

Figure 1. UV-vis spectra of IP_6@AgNPs with different concentrations of Fe^{3+}: (a) 0 μM, (b) 500 μM,(c) 1000 μM, and (d) 1200 μM.

to shed insight into the Fe^{3+} effect on the morphology of IP_6@AgNPs. Just a strong plasmon resonance peak at ∼390 nm of the silver colloid could be observed (Figure 1a), indicating that such a Ag colloid is spherically shaped,[38] which is consistent with the TEM image. In Figure 2a, the TEM image in the inset clearly shows that the synthesized colloid with highly dispersed state is wrapped by a thin layer of IP_6. The gap between both IP_6@AgNPs is ca. 5 nm. When IP_6@AgNPs colloid was added by increasing Fe^{3+} concentrations, the red shift of the UV-vis

dx.doi.org/10.1021/ic5003836 | Inorg. Chem. 2014, 53, 7227−7232

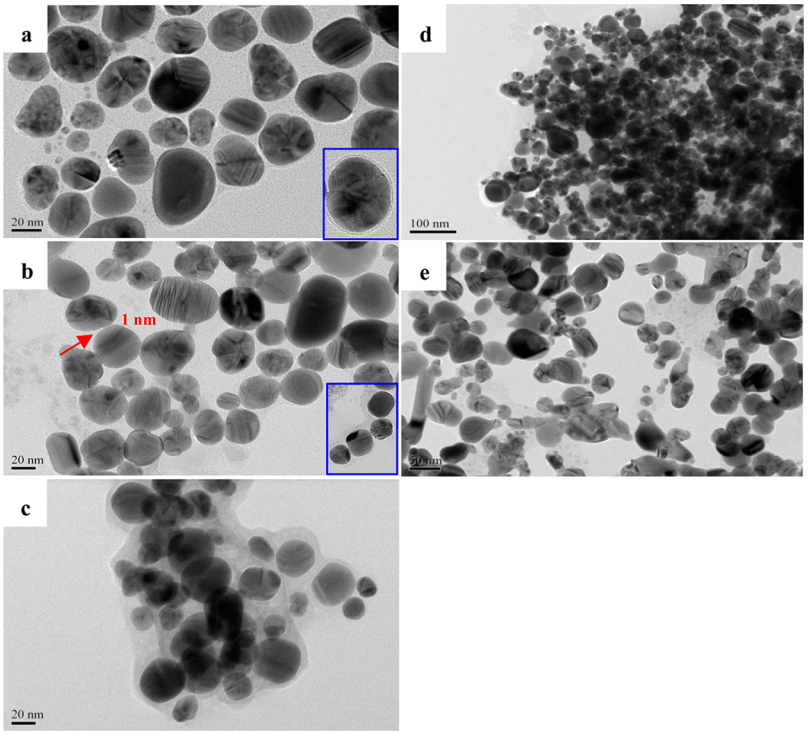

Figure 2. TEM images of the freshly prepared IP_6@AgNPs (a) without additional iron and with (b) 1000 μM Fe^{3+} and (c) 1200 μM Fe^{3+}; also shown are aged IP_6@AgNPs (d) without iron and (e) with 1000 μM Fe^{3+}.

band (see Figures 1b−1d) should be attributed to the formation of O···Fe···O between IP_6 and Fe^{3+}.[39] Aggregation of IP_6@AgNPs by Fe^{3+} could also be evidenced by the TEM image in Figure 2b. Under an optimal concentration of Fe^{3+}, the neighboring IP_6@AgNPs keep the certain gap ca. 1 nm (indication with red arrow in Figure 2b), which is denoted as a "hot spot"[40] and could greatly enhance SERS activity. However, after the addition of 10 μL of Fe^{3+} with the concentration exceeding 1000 μM, the UV-vis band becomes broader and the intensity decreases (Figure 1d). The TEM image in Figure 2c is recorded in the case of addition of Fe^{3+} at 1200 μM, showing that the distance of some of the neighboring IP_6@AgNPs becomes greater. The Raman signal of R6G mixed with the SERS substrate shown in Figure 2c is suppressed directly in the aforementioned SERS experiment (Figure 4e). The possible reason might be that more Fe^{3+} ions trend to break up the linking IP_6@AgNPs through O···Fe···O and then to form Fe···O bonds with individual IP_6@AgNPs. The schematic diagram of mechanism for Fe^{3+}-improved SERS activity of freshly prepared IP_6@AgNPs as well as Fe^{3+}-refreshed SERS activity of IP_6@AgNPs aged for one year is shown in Figure 3.

Fourier transform infrared (FT-IR) and XPS experiments are carried out to validate the effect of Fe^{3+} on the SERS activity of IP_6@AgNPs. In the FT-IR spectrum of Fe^{3+}−IP_6@AgNPs (Figure S1 in the Supporting Information), two new peaks at 835 and 1060 cm^{-1} appear compared with IP_6@AgNPs. According to the literature,[41,42] the peak at 835 cm^{-1} belongs to the Fe^{3+}−IP_6 compound and the peak at 1060 cm^{-1} is also attributed to the interaction of a trivalent metal cation with IP_6. In XPS spectrum of Fe^{3+}−IP_6@AgNPs, two peaks at 710 and 724 eV could be attributed to Fe^{3+} ion[43,44] (see Figure S2 in the Supporting Information). FT−IR and XPS observations further demonstrate that the due amount of Fe^{3+} could be used as

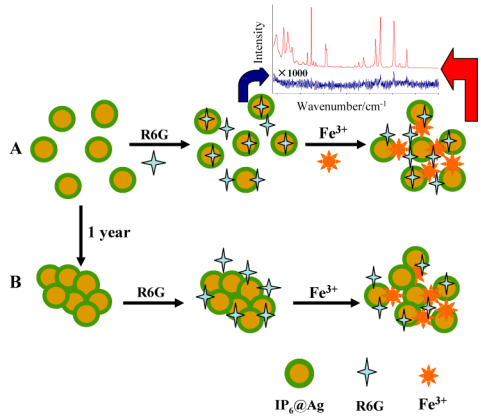

Figure 3. Schematic diagram of the enhancement mechanisms of Raman signals of R6G by adding due amounts of Fe^{3+} into (A) the freshly prepared silver colloid and (B) the aged silver colloid.

linkage agent to control the gaps between neighboring IP_6@AgNPs for producing the "hot spot".

The dynamic light scattering (DLS) measurements are also performed to demonstrate the sizes of IP_6@AgNPs without and with Fe^{3+} (see Figure S3 in the Supporting Information). The DLS results show that the average diameters of IP_6@AgNPs are ∼43 and 134 nm for the absence of Fe^{3+} and the presence of Fe^{3+}, respectively, also providing evidence that Fe^{3+} as the linkage agent make two or three neighboring nanoparticles closer.

3.2. Effect of Fe^{3+} Amount on SERS Activity of IP_6@AgNPs. 1 ×10^{-6} M R6G is used to investigate the enhancement effect on SERS activity of IP_6@AgNPs tuned by Fe^{3+} ions. As shown in Figure 4, at the beginning, the Raman signal of R6G is increased with the increase of Fe^{3+} concentration and the greatest level could be reached in the

dx.doi.org/10.1021/ic5003836 | Inorg. Chem. 2014, 53, 7227−7232

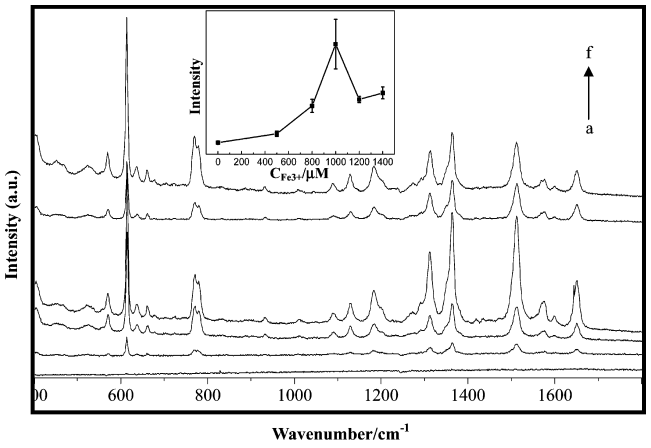

Figure 4. SERS spectra of 1×10^{-6} M R6G on IP_6@AgNPs at the addition of different Fe^{3+} concentrations: (a) 0 μM, (b) 500 μM, (c) 800 μM, (d) 1000 μM, (e) 1200 μM, (f) 1400 μM; inset shows the relationship between the additional amount of Fe^{3+} and SERS intensity of 1×10^{-6} M R6G with Fe^{3+}–IP_6@AgNPs (the observed band at 1512 cm^{-1}).

case of Fe^{3+} at 1000 μM, which might be due to producing the gaps ~1 nm among IP_6@AgNPs observed in TEM experiments and more Raman hot spots. More intuitively, the inset chart in Figure 4 illustrates the relationship between the Raman intensity of R6G at 1512 cm^{-1} and the addition of Fe^{3+}; the error bars are obtained from three measurements on different capillary tubes.

3.3. Enhancement Factor of SERS Substrates. Figure 5 shows the typical SERS spectra of R6G with various

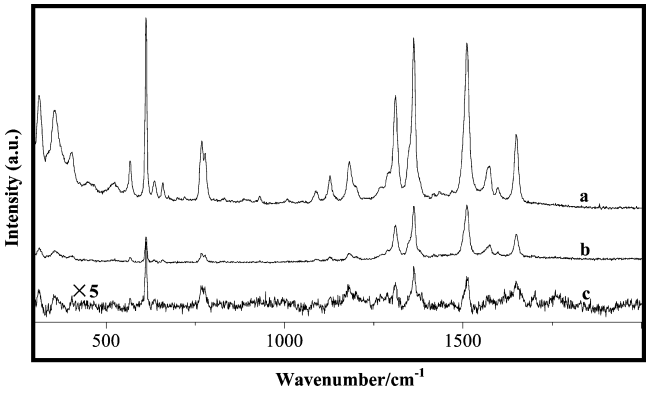

Figure 5. SERS spectra of the optimum Fe^{3+}–IP_6@AgNPs mixed with R6G: (a) 2.5×10^{-8} M, (b) 2.5×10^{-9} M, and (c) 2.5×10^{-10} M.

concentrations ranging from 2.5×10^{-8} M to 2.5×10^{-10} M. When the concentration of R6G is down to 2.5×10^{-10} M, its Raman peak could still be observed clearly, which could be regarded as the limit of detection (LOD) for R6G on Fe^{3+}–IP_6@AgNPs.

R6G and NF are used as SERS probe molecules (see Figures S4 and S5 in the Supporting Information) to calculate the enhancement factor (EF) values of IP_6@AgNPs and Fe^{3+}–IP_6@AgNPs following the equation below:[45]

$$EF = \frac{I_{SERS} C_{Raman}}{I_{Raman} C_{SERS}}$$

When R6G is used as a probe, the EF values of 1.2×10^2 and 6.6×10^6 from IP_6@AgNPs and Fe^{3+}–IP_6@AgNPs can be obtained, respectively. In the case of the NF probe, EF values of 6.3×10^3 and 7.4×10^6 from IP_6@AgNPs and Fe^{3+}–IP_6@AgNPs can be estimated, respectively. The above calculations demonstrate that Fe^{3+}–IP_6@AgNPs has higher SERS sensitivity than IP_6@AgNPs. In all, adding due amounts of Fe^{3+} into IP_6@AgNPs can promote the SERS activity of IP_6@AgNPs.

After storage for 1 year at room temperature, SERS activity of IP_6@AgNPs dramatically decreases (Figure 6a). Surprisingly,

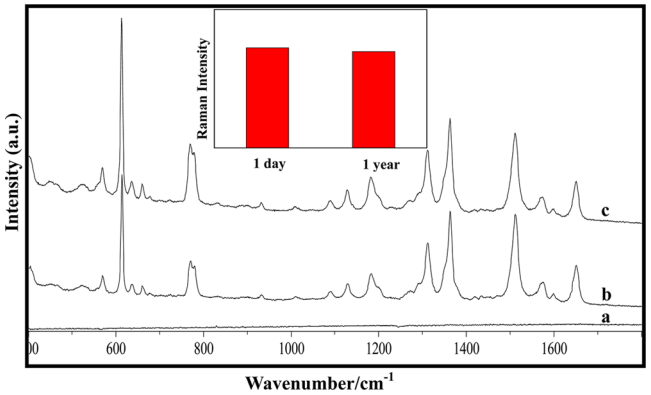

Figure 6. SERS spectra of R6G (1×10^{-6} M) mixed with IP_6@AgNPs which has been (a) stored for 1 year, (b) mixed with IP_6@AgNPs the same way as that for panel a and then adding due amounts of Fe^{3+}, and (c) mixed with IP_6@AgNPs which has been stored for 1 year and then adding due amounts of Fe^{3+}. Inset is the relationship between SERS intensity of 1×10^{-6} M R6G with the optimum Fe^{3+}–IP_6@AgNPs and the aging time of IP_6@AgNPs. The observed band is 1512 cm^{-1}.

mixed with 1000 μM Fe^{3+}, the one-year-aged IP_6@AgNPs could refresh Raman signal of 1×10^{-6} M R6G (Figure 6c), which is similar to the level of SERS intensity of 1×10^{-6} M R6G with the freshly prepared IP_6@AgNPs (Figure 6b). The inset histogram in Figure 6 as well as the TEM images in Figures 2d and 2e is much more clear observation for the recovery of SERS activity of aged IP_6@AgNPs aided by Fe^{3+}. The stability of unique AgNPs capped IP_6 endows the chance to tune the gaps of aged IP_6@AgNPs by adding suitable amounts of Fe^{3+} ions and realize the recovery of SERS activity.

3.4. Fe^{3+}–IP_6@AgNPs-Based SERS Measurement of Thymine. Figure 7 displays the SERS spectra of 2.5×10^{-3}

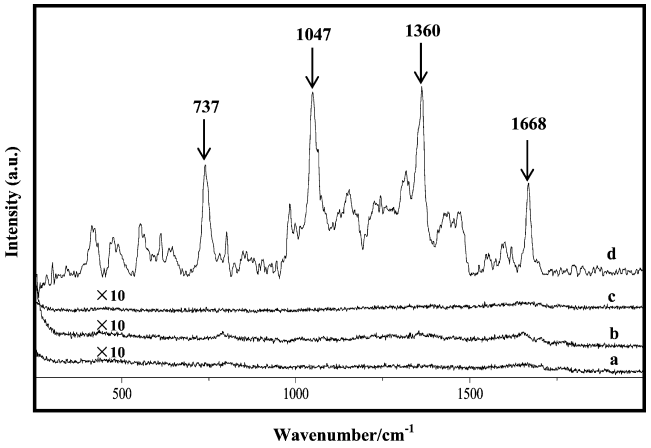

Figure 7. SERS spectrum of thymine (2.5×10^{-3} M) mixed with (a) AgNPs, (b) Fe^{3+}–AgNPs, (c) IP_6@AgNPs, and (d) the optimum Fe^{3+}–IP_6@AgNPs.

dx.doi.org/10.1021/ic5003836 | Inorg. Chem. 2014, 53, 7227–7232

Table 1. Assignments for SERS of Trace Thymine Aqueous Solution

Raman shift[a] (cm^{-1})	assignment
737 (s)	ring breathing and coupled to out-of-plane wag of N−H
1047 (vs)	C−H in methyl out-of-plane bending and N−H as well as C−H in-plane bending
1360 (vs)	N−H and C−H in-plane bending
1668 (s)	C═O stretching and coupled to N−H and C−H asymmetric bending

[a]vs, very strong; s, strong.

thymine mixed with different SERS substrates. Obviously, in the case of AgNPs synthesized via the method of Lee and Meisel,[37] the Raman signal of thymine is hardly seen at such low concentrations (Figure 7a), even after the addition of $FeCl_3$ (Figure 7b). For IP_6@AgNPs, the Raman signal of thymine is still invisible (Figure 7c). Only when using the Fe^{3+}−IP_6@AgNPs system, could the thymine Raman spectral bands clearly appear (Figure 7d). According to the literature,[46] assignments to SERS bands are tabulated in Table 1. A band at 737 cm^{-1} is attributed to ring breathing coupled to the out-of-plane wag of N−H in thymine. The band at 1047 cm^{-1} is from C−H in methyl out-of-plane bending and N−H as well as C−H in-plane bending. The SERS peak at 1360 cm^{-1} arises from N−H and C−H in-plane bending. The C═O stretching coupled to N−H and C−H asymmetric bending gives a Raman band centered at 1668 cm^{-1}. As a perspective, Fe^{3+}−IP_6@AgNPs is a suitable SERS substrate for Raman detection of biomolecules at a trace level.

4. CONCLUSIONS

In summary, improvement of the SERS activity of IP_6@AgNPs could be achieved by the addition of adequate amounts of Fe^{3+}. Fe^{3+}−IP_6@AgNPs with more Raman hot spots exhibits the high sensitivity of Raman scattering signals. Based on such Fe^{3+}−IP_6@AgNPs system, trace thymine could be detected. The SERS activity of IP_6@AgNPs aged for one year could be refreshed by adding due amounts of Fe^{3+}.

■ ASSOCIATED CONTENT

Supporting Information

This material is available free of charge via the Internet at http://pubs.acs.org.

■ AUTHOR INFORMATION

Corresponding Author

*Tel.: +86 21 64321701. Fax: +86 21 64322511. E-mail: haifengyang@yahoo.com.

Notes

The authors declare no competing financial interest.

■ ACKNOWLEDGMENTS

This work is supported by the National Natural Science Foundation of China (Grant No. 21073121), the Science Foundation of Shanghai Normal University (Grant No. SK201330), Foundation for Training Young Teachers in Shanghai Colleges and PCSIRT (IRT1269).

■ REFERENCES

(1) Fleischmann, M.; Hendra, P. J.; McQuillan, A. J. *Chem. Phys. Lett.* **1974**, *26*, 163−166.
(2) Vongsvivut, J.; Robertson, E. G.; McNaughton, D. *J. Raman Spectrosc.* **2010**, *41*, 137−1148.
(3) Alvarez−Puebla, R. A.; Aroca, R. F. *Anal. Chem.* **2009**, *81*, 2280−2285.
(4) Culha, M.; Stokes, D.; Allain, L. R.; Vo Dinh, T. *Anal. Chem.* **2003**, *75*, 6196−6201.
(5) Liu, R. M.; Zi, X. F.; Kang, Y. P.; Si, M. Z.; Wu, Y. C. *J. Raman Spectrosc.* **2011**, *42*, 137−144.
(6) Wang, Y. Q.; Ma, S.; Yang, Q. Q.; Li, X. J. *Appl. Surf. Sci.* **2012**, *258*, 5881−5885.
(7) Keating, C. D.; Kovaleski, K. K.; Natan, M. J. *J. Phys. Chem. B* **1998**, *102*, 9414−9425.
(8) Van Lierop, D.; Larmour, I. A.; Faulds, K.; Graham, D. *Anal. Chem.* **2013**, *85*, 1408−1414.
(9) Brown, R. J. C.; Wang, J.; Tantra, R.; Yardley, R. E.; Milton, M. J. T. *Faraday Discuss.* **2006**, *132*, 201−213.
(10) Fu, C. Y.; Kho, K. W.; Dinish, U. S.; Koh, Z. Y.; Malini, O. *J. Raman Spectrosc.* **2012**, *43*, 977−985.
(11) MacLaughlin, C. M.; Mullaithilaga, N.; Yang, G. S.; Ip, S. Y.; Wang, C.; Walker, G. C. *Langmuir* **2013**, *29*, 1908−1919.
(12) Li, J. F.; Huang, Y. F.; Ding, Y.; Yang, Z. L.; Li, S. B.; Zhou, X. S.; Fan, F. R.; Zhang, W.; Zhou, Z. Y.; Wu, D. Y. *Nature* **2010**, *464*, 392−395.
(13) Zhang, J. T.; Li, X. L.; Sun, X. M.; Li, Y. D. *J. Phys. Chem. B* **2005**, *109*, 12544−12548.
(14) Halvorson, R. A.; Vikesland, P. J. *Environ. Sci. Technol.* **2010**, *44*, 7749−7755.
(15) Itoh, T.; Hashimoto, K.; Biju, V.; Ishikawa, M.; Wood, B. R.; Ozaki, Y. *J. Phys. Chem. B* **2006**, *110*, 9579−9585.
(16) Shalaev, V. M.; Sarychev, A. K. *Phys. Rev. B* **1998**, *57*, 13265−13288.
(17) Kahl, M.; Voges, E. *Phys. Rev. B* **2000**, *61*, 14078−14088.
(18) Meyer, S. A.; Le Ru, E. C.; Etchegoin, P. G. *Anal. Chem.* **2011**, *83*, 2337−2344.
(19) Etchegoin, P.; Cohen, L.; Hartigan, H.; Brown, R.; Milton, M.; Gallop, J. *J. Chem. Phys.* **2003**, *119*, 5285−5289.
(20) Camden, J. P.; Dieringer, J. A.; Wang, Y. M.; Masiello, D. J.; Marks, L. D.; Schatz, G. C.; Van Duyne, R. P. *J. Am. Chem. Soc.* **2008**, *130*, 12616−12617.
(21) Lim, D. K.; Jeon, K. S.; Kim, H. M.; Nam, J. M.; Suh, Y. D. *Nature materials* **2009**, *9*, 60−67.
(22) Nie, S.; Emory, S. R. *Science* **1997**, *275*, 1102−1106.
(23) Michaels, A. M.; Jiang, J.; Brus, L. *J. Phys. Chem. B* **2000**, *104*, 11965−11971.
(24) Hu, M.; Ou, F. S.; Wu, W.; Naumov, I.; Li, X. M.; Bratkovsky, A. M.; Williams, R. S.; Li, Z. Y. *J. Am. Chem. Soc.* **2010**, *132*, 12820−12822.
(25) Chen, X. Y.; Wen, Y.; Wang, N.; Gu, K.; Yang, H. F. *Nanotechnology* **2011**, *22*, 205603.
(26) Charles Cao, Y. W.; Jin, R. C.; Mirkin, C. A. *Science* **2002**, *297*, 1536−1540.
(27) Sun, L. L.; Song, Y. H.; Wang, L.; Guo, C. L.; Sun, Y. J.; Liu, Z. L.; Li, Z. *J. Phys. Chem. C* **2008**, *112*, 1415−1422.
(28) Ahonen, P.; Laaksonen, T.; Nykanen, A.; Ruokolainen, J.; Kontturi, K. *J. Phys. Chem. B* **2006**, *110*, 12954−12958.
(29) Lin, X.; Hasi, W. L. J.; Lou, X. T.; Lin, S.; Yang, F.; Jia, B. S.; Cui, Y.; Ba, D. X.; Lin, D. Y.; Lu, Z. W. *J. Raman Spectrosc.* **2014**, *45*, 162−167.
(30) Hu, J. W.; Zhao, B.; Xu, W. Q.; Fan, Y. G.; Li, B.; Ozaki, Y. *Langmuir* **2002**, *18*, 6839−6844.
(31) Wang, X. K.; Chen, L.; Fu, X. L.; Chen, L. X.; Ding, Y. J. *ACS Appl. Mater. Interfaces* **2013**, *5*, 11059−11065.

(32) Yang, H. F.; Feng, J.; Liu, Y. L.; Yang, Y.; Zhang, Z. R.; Shen, G. L.; Yu, R. Q. *J. Phys. Chem. B* **2004**, *108*, 17412−17417.
(33) Wang, N.; Yang, H. F.; Zhu, X.; Zhang, R.; Wang, Y.; Huang, G. F.; Zhang, Z. R. *Nanotechnology* **2009**, *20*, 315603.
(34) Begley, T. P. *Acc. Chem. Res.* **1994**, *27*, 394−401.
(35) Kim, S. T.; Sancar, A. *Biochemistry* **1991**, *30*, 8623−8630.
(36) Da Silva, A.; Condessa, G. R. *Quím Nova* **2008**, *31*, 1686−1690.
(37) Lee, P. C.; Meisel, D. *J. Phys. Chem.* **1982**, *86*, 3391−3395.
(38) Liu, Z.; Xing, Z.; Zu, Y.; Tan, S.; Zhao, L.; Zhou, Z.; Sun, T. *Mater. Sci. Eng., C* **2012**, *32*, 811−816.
(39) Yu, S.; Cowieson, A.; Gilbert, C.; Plumstead, P.; Dalsgaard, S. *J. Anim. Sci.* **2012**, *90*, 1824−1832.
(40) Kleinman, S. L.; Frontiera, R. R.; Henry, A. I.; Dieringer, J. A.; Van Duyne, R. P. *Phys. Chem. Chem. Phys.* **2013**, *15*, 21−36.
(41) He, Z. Q.; Wayne Honeycutt, C.; Zhang, T. Q.; Bertsch, P. M. *J. Environ. Qual.* **2006**, *35*, 1319−1328.
(42) Jiang, G. P.; Qiao, J. L.; Hong, F. *Int. J. Hydrogen Energy* **2012**, *37*, 9182−9192.
(43) Graat, P. C. J.; Somers, M. A. J. *Appl. Surf. Sci.* **1996**, *100/101*, 36−40.
(44) Yamashita, T.; Hayes, P. *Appl. Surf. Sci.* **2008**, *254*, 2441−2449.
(45) Zhang, J.; Qu, S.; Zhang, L.; Tang, A.; Wang, Z. *Spectrochim. Acta, Part A* **2011**, *79*, 625−630.
(46) Zhang, L.; Li, Q. Q.; Tao, W.; Yu, B. H.; Du, Y. P. *Anal. Bioanal. Chem.* **2010**, *398*, 1827−1832.

dx.doi.org/10.1021/ic5003836 | *Inorg. Chem.* 2014, 53, 7227−7232